Performance Characteristics of Electron Transfer Dissociation Mass Spectrometry*[S]

David M. Good‡§, Matthew Wirtala‡, Graeme C. McAlister‡§, and Joshua J. Coon‡¶‖

We performed a large scale study of electron transfer dissociation (ETD) performance, as compared with ion trap collision-activated dissociation (CAD), for peptides ranging from ~1000 to 5000 Da ($n \sim 4000$). These data indicate relatively little overlap in peptide identifications between the two methods (~12%). ETD outperformed CAD for all charge states greater than 2; however, regardless of precursor charge a linear decrease in percent fragmentation, as a function of increasing precursor *m/z*, was observed with ETD fragmentation. We postulate that several precursor cation attributes, including peptide length, charge distribution, and total mass, could be relevant players. To examine these parameters unique ETD-identified peptides were sorted by length, and the ratio of amino acid residues per precursor charge (residues/charge) was calculated. We observed excellent correlation between the ratio of residues/charge and percent fragmentation. For peptides of a given residue/charge ratio, there is no correlation between peptide mass and percent fragmentation; instead we conclude that the ratio of residues/charge is the main factor in determining a successful ETD outcome. As charge density decreases so does the probability of non-covalent interactions that can bind a newly formed c/z-type ion pair. Recently we have described a supplemental activation approach (ETcaD) to convert these non-dissociative electron transfer product ions to useful c- and z-type ions. Automated implementation of such methods should remove this apparent precursor *m/z* ceiling. Finally, we evaluated the role of ion density (both anionic and cationic) and reaction duration for an ETD experiment. These data indicate that the best performance is achieved when the ion trap is filled to its space charge limit with anionic reagents. In this largest scale study of ETD to date, ETD continues to show great promise to propel the field of proteomics and, for small- to medium-sized peptides, is highly complementary to ion trap CAD. ***Molecular & Cellular Proteomics 6:1942–1951, 2007.***

Electron transfer dissociation (ETD),[1] a relatively new peptide/protein fragmentation method, holds great promise to advance the field of protein mass spectrometry (1–3). As compared with the conventional technique, collision-activated dissociation (CAD), ETD offers a more robust method to characterize post-translational modifications (PTMs) and to interrogate large peptides or even whole proteins (4–7). Because of these attributes and the fact that it generates c- and z-type products, instead of b- and y-type, many propose that ETD is highly complementary to CAD. ETD reactions, of course, are generally conducted within the confines of ion trap mass spectrometers where sequential CAD and ETD experiments are easily performed. Most proteomics experiments, however, are coupled with on-line chromatographic separations, and analysis time, per peptide, is ideally minimized to increase dynamic range (8). Thus, to extract the most information from a given experiment, knowledge of how these two dissociation techniques complement one another is critical.

As CAD has been extensively studied for several years, most MS proteomics practitioners have a good sense of how to best utilize the method (9–12). Trypsin, for example, is the enzyme of choice for CAD-based tandem MS approaches. Cleaving proteins C-terminal to Lys or Arg residues ensures that the resulting peptides are relatively short (~10–15 residues) and that they do not contain an internal basic residue, which could prevent random backbone protonation and, ultimately, successful sequencing. Many PTMs, however, are especially labile under CAD conditions; in fact, ETD was initially developed to enable the large scale characterization of protein phosphorylation (6). Besides accounts on its value for either PTM characterization or the interrogation of high mass species, few ETD works have been reported.

Several recent studies indicate that ETD is particularly ineffective for the dissociation of peptide dications (13, 14). Recent work in our own laboratory confirms this but also revealed some interesting trends (15). For example, regardless of precursor *m/z* value, doubly protonated precursor cations rarely produced complementary product ion pairs. The number of observed c- and z-type product ions, however, did decrease linearly with increasing precursor *m/z* for all peptide dications. This problem was remedied by the application of a supplemental collisional activation step (ETcaD) (15), a process that was inspired by prior reports of activated ion electron capture dissociation (16–20). Here we asked

From the Departments of ‡Chemistry and ¶Biomolecular Chemistry, University of Wisconsin, Madison, Wisconsin 53706

Received, February 16, 2007, and in revised form, June 12, 2007
Published, MCP Papers in Press, August 1, 2007, DOI 10.1074/mcp.M700073-MCP200

[1] The abbreviations used are: ETD, electron transfer dissociation; CAD, collision-activated dissociation; PTM, post-translational modification; LTQ, linear quadrupole ion trap; ETcaD, supplemental activation; AGC, automated gain control; CI, chemical ionization; DTA, Data (file name extension); NCI, negative chemical ionization; GdmHCl, guanidinium hydrochloride; ET, electron transfer.

whether precursor cations in higher charge states (*i.e.* ≥3) show similar trends upon ETD fragmentation, and if so, is ETcaD an effective remedy? To answer these questions, we examined the performance of ETD for the characterization of small- to medium-sized, unmodified peptides from complex mixtures (*i.e.* those resulting from either trypsin or Lys-C). Sequential tandem MS events were used to toggle between ETD and ion trap CAD fragmentation. From these datasets we determined the extent of complementarity and the overall performance of the two methods. ETD-identified peptides were categorized by precursor mass, charge, and/or length and were examined for the observed percent fragmentation. Finally, we evaluated the role of several ETD parameters and their impact on the resulting tandem mass spectra, including magnitude of the anionic and cationic populations and reaction duration.

EXPERIMENTAL PROCEDURES

Sample Preparation—Yeast ("wild type" S288C strain, α mating type, diploid, *SUC2 mal mel gal2 CUP1*) was cultured on yeast nitrogen base (Difco) without amino acids and ammonium sulfate with 2% glucose. The solution was held at 30 °C and shaken overnight. After ~18 h, this solution was transferred to a Fernbach flask where it was shaken for ~18 h at 30 °C. The resulting solution was spun down and washed with deionized water, and a lysis buffer (50 mM Tris base, 0.3 M sucrose, 5 mM Na_2EDTA, 1 mM EDTA-free acid, 1 mM PMSF from 100 mM isopropyl alcohol stock, pH to 7.5 with HCl) was added. For lysis, the yeast cells were sonicated for ~3 min in 1-min intervals. Organelles and membranes were pelleted using centrifugation (~2000 and ~100,000 × *g*, respectively). After an acetone precipitation, the soluble proteins were redissolved in 6 M guanidinium hydrochloride (GdmHCl). The protein extracts were equally aliquoted and digested with either trypsin (in 1 M GdmHCl for ~18 h at pH ~8) or Lys-C (0.5 M GdmHCl for ~18 h at pH ~8). *Arabidopsis* plants were grown, and a whole cell lysate was prepared as described above. Trypsin and Lys-C digests were performed as outlined above for yeast (15).

Chromatography—Yeast and *Arabidopsis* digests were loaded onto separate 360 × 75-μm monolithic microcapillary precolumns, which were fritted (Lichrosorb Si60, EM Separations Technology, Gibbstown, NJ) and packed in house with reversed-phase C_{18} material (Alltima C_{18} 5-μm beads from Alltech Associates, Inc., Deerfield, IL). To each precolumn was attached a separate 360 × 50-μm microcapillary column, again packed with reversed-phase C_{18} material, by a butt-joint with Teflon® tubing. These columns had integrated ESI tips created by a laser puller (Model P-2000, Sutter Instrument Co., Novato, CA) as described elsewhere (21). Following sample loading (~5–10 pmol of total peptide), peptides were gradient-eluted (2-h gradient; Model 1100, Agilent Technologies, Palo Alto, CA) directly into an ETD-enabled linear ion trap mass spectrometer (Finnigan LTQ, Thermo Fisher, San Jose, CA).

Mass Spectrometry—A Finnigan LTQ was modified to accept a chemical ionization (CI) source on the rear of the device opposing the factory nanospray source. Negative CI was used to produce radical anions of fluoranthene, which were introduced through a batch inlet consisting of a gas chromatograph oven and heated transfer line (SRI Instruments, Torrance, CA). Once in the CI source, fluoranthene neutral molecules were ionized via electron capture as described previously (5, 6). The LTQ was also adapted to apply a radio frequency trapping voltage to the end lenses of the linear ion trap. By applying radio frequency voltages in both the radial (applied to the quadrupole rods) and axial (applied to the end lenses) directions without additional direct current offsets, ions of opposing charge can be trapped in the same space at the same time (*i.e.* charge sign-independent trapping). Peptide cations were first introduced into the front of the linear trap, isolated, and then stored while fluoranthene anions were introduced into the trap through the rear. The ETD-enabled Finnigan LTQ places a quadrupole mass filter between the CI source and LTQ to selectively inject only radical anions of fluoranthene (*m/z* 202). Both the anion and cation populations were regulated by use of an integrated automatic gain control (AGC) function. A data-dependent acquisition method was written to interrogate the five most intense precursor ions, as identified from each full MS scan, by both ion trap CAD and ETD (two separate sequential events). For CAD, the AGC target was set to inject ~40,000 peptide cations. Dissociation was accomplished at a *q* value of 0.25 with an energy of 35% (normalized collision energy) for 30 ms (single scan). For ETD, the precursor cation AGC target was set at 80,000, whereas a value of 100,000 was used for the anion population. Ion/ion reaction duration was fixed at 80 ms.

Resultant data files were used to create DTA files that were then separated by fragmentation method, *i.e.* CAD or ETD. Database correlation was performed with the Open Mass Spectrometry Search Algorithm (free at the National Center for Biotechnology Information (NCBI), National Institutes of Health, Bethesda, MD) (22). All searches were performed as both organism- and enzyme-specific with nonredundant libraries for yeast and *Arabidopsis* provided by NCBI. The product ion mass tolerance was set at ±0.5 Da, the precursor ion mass tolerance was ±1.2 Da, and there was no scaling of precursor mass tolerance with charge. Returned matches with probability scores less than 0.01 were short-listed for subsequent manual inspection. All short-listed sequences were inspected for goodness of fit: if the major product ions could not be manually explained by the proposed sequence the identification was rejected.

RESULTS

Global Comparison of ETD with Ion Trap CAD—Sequential ETD and CAD analyses, *i.e.* back-to-back tandem MS events, were performed, in a data-dependent fashion, on peptides derived from multiple complex mixtures as they eluted from a reversed-phase chromatographic separation. From these analyses 3287 unique peptides (0.48% false positive/negative rate using concatenated forward and reversed database search (23)) were identified by use of an automated database correlation algorithm (Open Mass Spectrometry Search Algorithm; expectation value cutoff of 0.01) and were individually confirmed by manual inspection of each. All identified peptides were compared within a species (*e.g.* yeast peptides identified from a Lys-C digestion were compared with those identified from a tryptic digestion), and if several matches existed, only one was counted toward the total. This insured only one peptide identification per unique amino acid sequence for each of the organisms. Of the 3287 unique peptides sequenced, 1301 and 1986 were identified from the corresponding ETD and CAD spectra, respectively; however, to consider the effect of precursor charge (*z*), multiple peptide identifications for the same amino acid sequence were allowed given that each of the identifications was derived from a different precursor charge state. These criteria expanded the number of sampled peptides (or more accurately, the number of unique precursor *m/z* values characterized) to 3866

TABLE I
Total peptide identifications (IDs) sorted by precursor charge state and fragmentation method

Precursor charge state	No. peptides identified by ion trap CAD	No. peptides identified by ETD	No. overlapping IDs
+1	5	0	0
+2	1224	6	6
+3	698	946	362
+4	130	324	86
+5	8	59	6
+6	0	6	0
Total	2065	1341	460

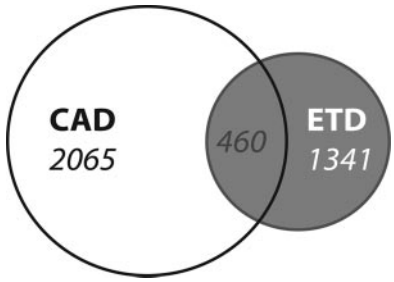

FIG. 1. **Of the 3866 total peptides sequenced, there was only a ~12% overlap in identifications from ion trap CAD and ETD.**

with the relative breakdown of charge state and overlap provided in Table I (for a complete list see supplemental data).

Surprisingly little overlap is observed among the peptides identified following activation by these techniques, only ~12% (Fig. 1). Inspection of Table I, however, reveals some expected trends. First, we note that CAD performs best with doubly protonated precursors, yielding 1224 unique sequences as compared with six for ETD. This number represents nearly half of all identifications derived from the CAD spectra. ETD, on the other hand, harbored 946 unique sequences from triply protonated precursors and outperformed CAD in every charge state with the exception of $z = 1$ or 2. A number of higher charge peptides were identified using ETD, but triply protonated precursors constituted the majority (359 peptides with $z > 4$). From Table I, the inability of ETD to effectively dissociate peptide dications is palpable. Recently our group has reported on the use of ETD to dissociate doubly protonated peptides (15). As compared with ion trap CAD (for peptide dications), we found that ETD rarely resulted in the formation of complementary product ion pairs even in cases where high fragmentation efficiency was observed. From the 755 peptide dications studied, however, a strong dependence on precursor *m/z* was observed (15). Increasing precursor *m/z* correlated with a linear decrease in both percent fragmentation and peptide sequence coverage. For electron-based methods of fragmentation, including ETD, decreasing percent fragmentation is accompanied by a partitioning from direct dissociation (ETD, formation of c- and z-type product ions) to charge reduction without fragmentation (non-dissociative ET) (13–15, 24–30). Here we asked whether similar trends exist for peptide precursor cations having a charge of 3 or higher; and, if so, what are the attributes of a precursor cation that lead to a successful ETD outcome?

To examine the effects of charge and precursor *m/z,* the percent fragmentation for the identified peptides (as outlined in Table I) were compared for both CAD and ETD fragmentation. Here percent fragmentation is defined as the number of observed c- and z-type fragment ions, for a given sequence, divided by the theoretical number of fragment ions (*e.g.* a 10-residue peptide could produce 18 c- and z-type fragment ions). Although it is not generally observed with electron-based fragmentation methods, N-terminal proline cleavage was included as a possible fragmentation channel (31). Fig. 2 plots each of the 3866 unique identified precursor *m/z* values and displays the observed percent fragmentation for each. From these data we notice a striking trend for ETD: percent fragmentation decreases linearly with increasing precursor *m/z* regardless of precursor charge. Few peptides having precursor *m/z* values exceeding ~850 were identified via ETD fragmentation presumably due to the lack of a sufficient number of c- and z-type product ions for successful database correlation. Note that a similar, but much subtler, trend was also observed from the ion trap CAD spectra. For peptide precursor ions having a charge of at least 3 and *m/z* values up to ~850, ETD is highly effective, inducing significantly higher percent fragmentation values than ion trap CAD. This is apparent both from the data presented in Fig. 2 and from the higher numbers of identified peptides in all charge states greater than 2.

In a sense, the above data suggest the existence of a precursor *m/z* ceiling for a successful ETD event. Steps to remove, or at least raise, this ceiling will require a good understanding of the responsible precursor cation characteristics. The data from Fig. 2 only considers precursor *m/z*, but we postulated that other precursor cation attributes such as peptide length, charge distribution, and total mass could be relevant players. To examine these parameters we sorted the unique ETD-identified peptides by length and calculated the ratio of amino acid residues per precursor charge (residue/charge). Fig. 3, *Panel A*, displays the percent fragmentation of each peptide plotted as a function of residue/charge for precursors having charges of 3, 4, and 5. Fig. 3, *Panels B–D*, display each of these charge state series separately. From these data we observe excellent correlation between the ratio of residue/charge and percent fragmentation. For a given residue/charge ratio, precursor charge has virtually no impact on the ETD outcome. Note the pentuply charged series shows a slightly lowered percent fragmentation as compared with the others; however, we suspect this is an artifact of low *m/z* resolution and limited *m/z* range of the mass analyzer, not ETD. Next we examined the role of peptide mass by sorting unique identified peptides first by precursor charge and second by length. Here we held peptide length and precursor

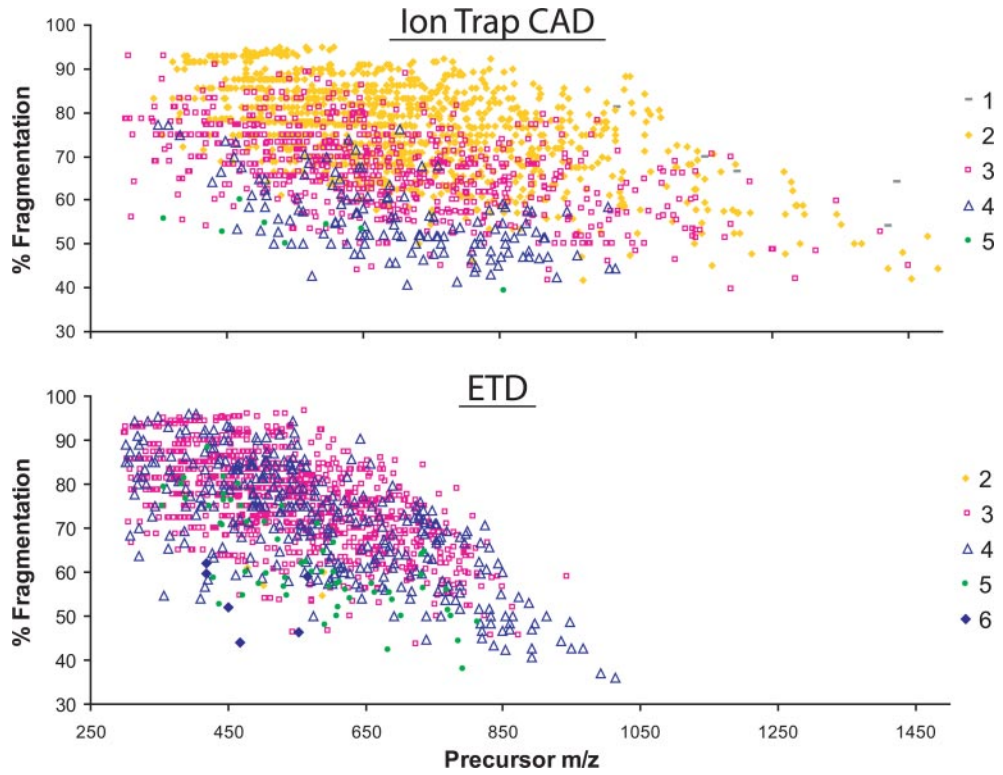

FIG. 2. **Percent fragmentation (number of observed fragment ions/number of theoretical fragment ions) is highly dependent on precursor *m/z*, especially for ETD.** Plotted here is the calculated percent fragmentation for each identified peptide as a function of precursor *m/z*, fragmentation method, and charge state.

charge constant, essentially fixing the ratio of residue/charge, to test whether the presence of heavy amino acids, for example, lower the observed percent fragmentation. Fig. 3, *Panels E–H*, display these results for 11-, 14-, 16-, and 18-residue peptides, respectively. For peptides of a given residue/charge ratio, there is no correlation between peptide mass and percent fragmentation; instead the relationship between precursor *m/z* and percent fragmentation displayed in Fig. 2 results from correlation of mass and amino acid count (*i.e.* most 11-residue peptides vary in mass by only 10–30%). From these data we propose that the ratio of residues/charge is the main factor in determining a successful ETD outcome.

An assumption of the ETD to CAD comparison detailed above is that the relative intensity of the precursor ion does not substantially change from one scan to the next. Each scan event persists for ~350 ms, which is far shorter than the average chromatographic peak width of ~ 20 s; however, to ensure this assumption is valid, we performed two additional data-dependent analyses with back-to-back sequential tandem MS using either ETD or CAD, *i.e.* ETD followed by ETD or CAD followed by CAD of the yeast tryptic digest. To examine variation in spectral quality we correlated partner spectra with themselves and randomly chosen tandem MS spectra (dot product method, $n = 100$ for each) (32). With this algorithm, completely identical spectra are scored at 1.0, whereas a score of 0.0 indicates no conservation of spectral features. Correlation scores for spectra resulting from isolation of the same precursor but in consecutive scans were 0.87 ± 0.03 for CAD and 0.92 ± 0.02 for ETD, indicating a high degree of similarity between sequential tandem MS events. The average correlation score for a spectrum compared with all other spectra within the list, except for itself and its partner, was 0.25 ± 0.01 for ETD and 0.30 ± 0.01 for CAD. Using Student's *t* test, the mean correlation score of consecutive spectra (partners) was compared with the mean correlation score for spectra compared with all others except for itself and its partner. The comparison resulted in *t* values of 33.3 for CAD and 60.0 for ETD, which are both well outside the range of values where the null hypothesis could be accepted; therefore, there is a statistically significant difference between the similarity of spectra resulting from consecutive isolation and fragmentation of the same precursor, by either fragmentation method, and those resulting from isolation of differing precursor *m/z* values. In short, the consecutive dissociation events generated highly similar product ion spectra for both ETD- and CAD-type fragmentation (see Supplemental Fig. 1 for examples).

Elevating the ETD Precursor m/z Limit—Our observations are consistent with the concept that non-covalent interactions lower ECD fragmentation efficiencies (18). Such interactions are heightened as the ratio of residue/charge increases, *i.e.* low charge density induces a more folded cationic structure

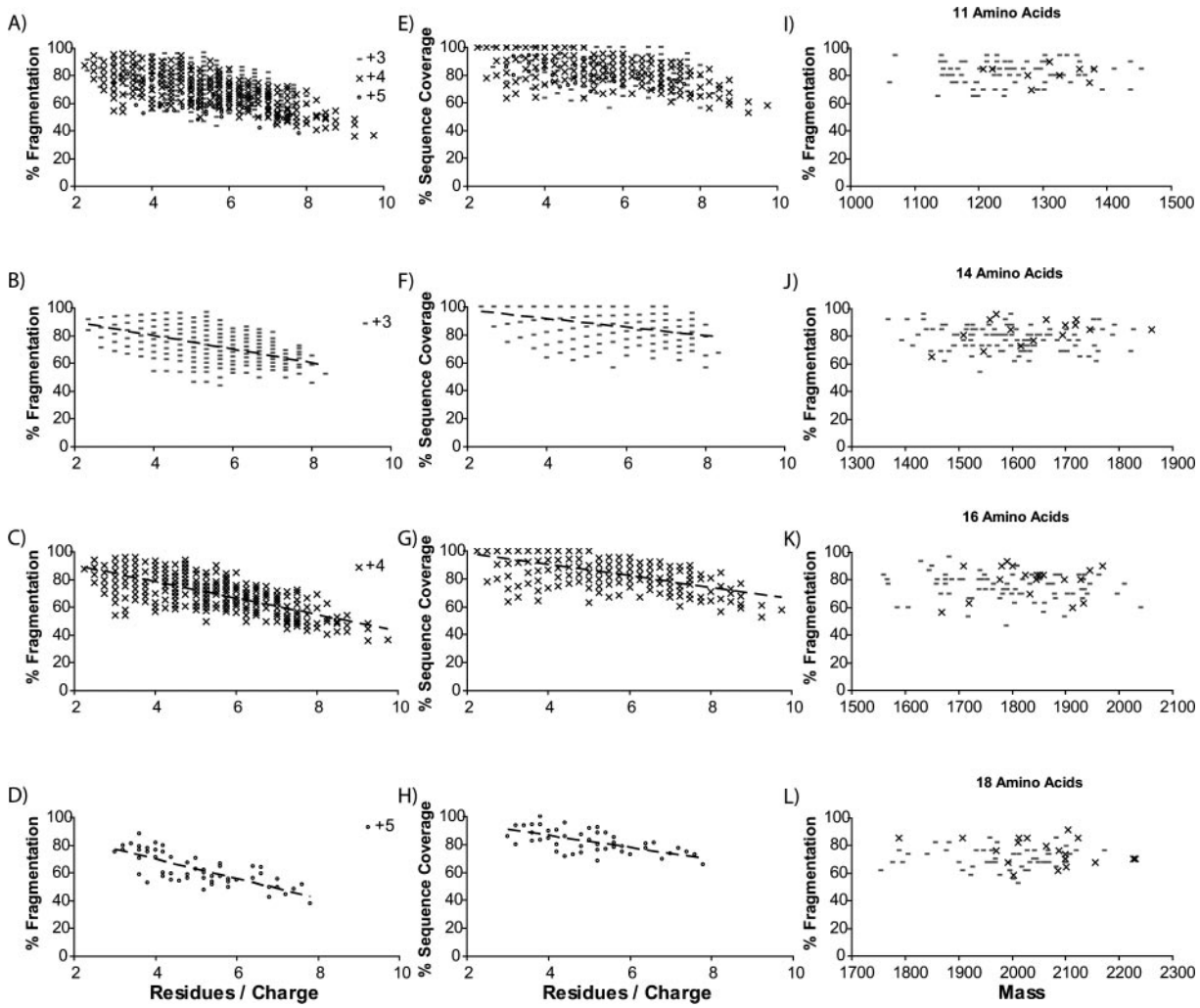

FIG. 3. **The residue/charge ratio is the main factor in determining a successful ETD outcome.** *Panels A–D* display the decrease in percent fragmentation (by ETD) as the ratio of residue/charge increases for precursor cations having charges of 3, 4, and 5. Although percent fragmentation decreases rapidly, the percent sequence coverage (number of backbone bonds cleaved/number of backbone bonds) is much less affected (*Panels E–H*). *Panels I–L* indicate that total mass (for fixed residue/charge ratio) has relatively little effect on percent fragmentation. The *dashed lines* in *Panels B–H* are to guide the eye.

that can remain bound, through non-covalent interactions, even after backbone bond cleavage. One approach to destroy non-covalent interactions, and thereby increase ECD fragmentation efficiency, is to heat, typically with collisions or photons, the cationic precursor species prior to or during the electron capture period (16–18). Electron transfer reactions, however, occur at pressures ~6 orders of magnitude higher where the effects of heating before or during reaction periods are negated by rapid collisional cooling. Instead we have recently implemented an approach that targets the non-dissociated electron transfer product for gentle collisional activation (ETcaD) (15). This approach was found to near exclusively convert the charge-reduced ET product of peptide dications to c- and z-type product ions, presumably by disrupting the tethering non-covalent linkages, with high efficiency (~80%). Automated implementation of ETcaD harbored a significant increase in percent fragmentation for doubly protonated peptide precursors ($n = 755$) and resulted in a mean percent sequence coverage (89%) that bested ion trap CAD (77%).

Here we propose ETcaD as a possible route to elevate the precursor *m/z* limit for higher charge precursor cations. Fig. 5, *Panels A–C*, display ETD product ion spectra resulting from fragmentation of the standard adrenocorticotropic hormone peptide cation having charges of 6, 5, and 4, respectively. Consistent with the large scale dataset plotted in Fig. 2, the extent of direct c- and z-type product ion formation (unlabeled peaks) decreases with increasing precursor *m/z* (57, 39, and 26% fragmentation, respectively). Also note the increase in the non-dissociative product ions. To test our hypothesis we isolated and gently collisionally activated the undissociated double electron transfer charge-reduced product ion ([M +

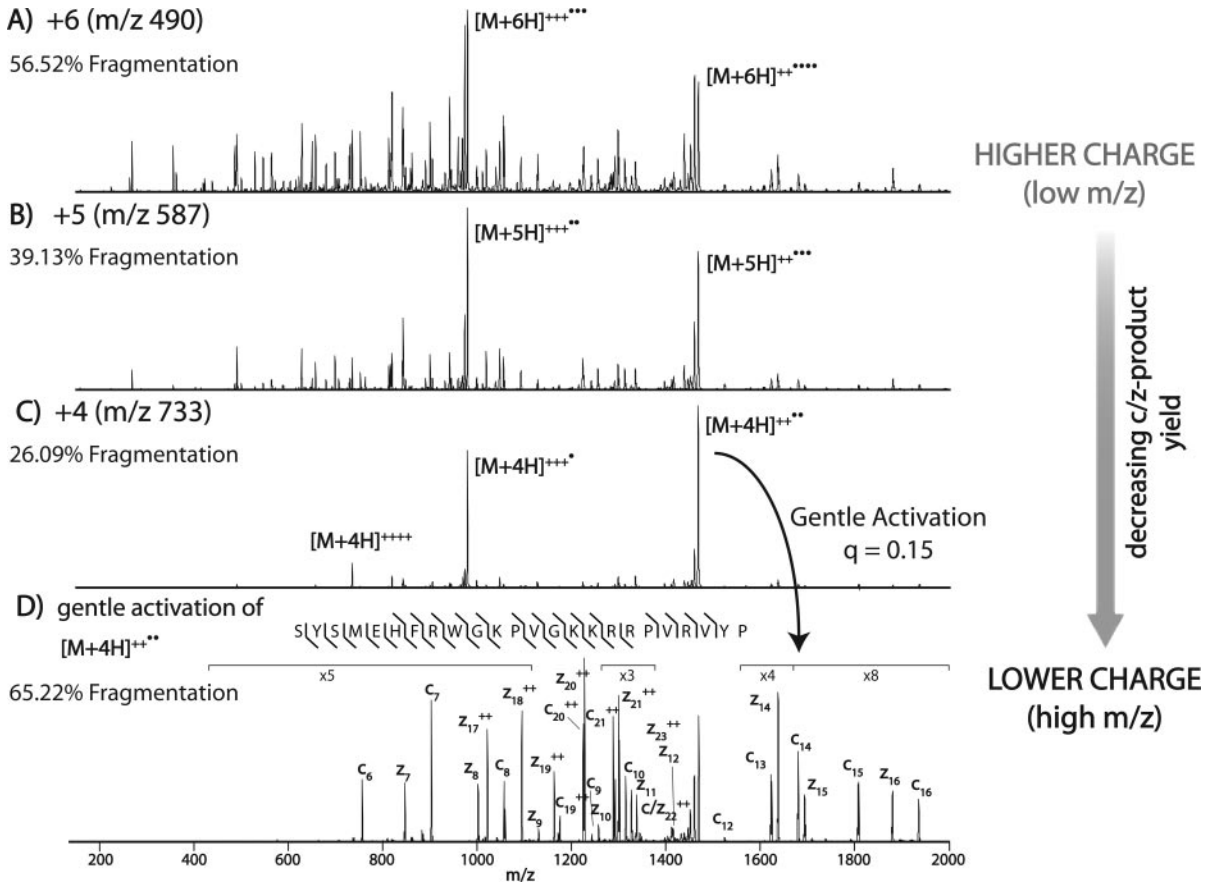

FIG. 4. ETD dissociation of +6, +5, and +4 charge states of the 24-residue adrenocorticotropic hormone peptide (*Panels A*, *B*, and *C*, respectively) is shown. Note the partitioning between direct fragmentation and the formation of non-dissociative ET with decreasing precursor charge. Application of a gentle collisional activation step to an isolated, non-dissociative ET product, $[M + 4H]^{+\bullet}$, results in exclusive formation of c/z-type products (*Panel D*).

$4H]^{2+\bullet}$) of the quadruply charged precursor cation. ETcaD results in the formation of an extensive series of c- and z-type product ions to yield a percent fragmentation of 65, an increase over the already good ETD performance of the +6 precursor (Fig. 4, *Panel A*). From these results we conclude that ETcaD is a viable approach to increase ETD fragmentation efficiency for precursor cations of charge 3 or higher.

Automated implementation of ETcaD for precursor cations having charges of 3 or higher presents some challenges. For example, there will be $z - 1$ (z = precursor charge) charge-reduced, non-dissociated product ions to activate by ETcaD. Precursor cations having a charge of 3 or higher will, of course, have at least two species to target for follow-up activation. Activating multiple species is not necessarily a problem; however, determining the non-dissociative target *m/z* values requires *a priori* knowledge of precursor charge state. On low resolution ion trap instruments obtaining such knowledge will likely require an additional survey scan. And for highest efficiency, isolation of the individual charge-reduced peaks should not be performed; there is no need to eliminate the c- and z-type products formed directly from electron transfer or to discard non-dissociative product species. With these data, we have begun work to automatically implement ETcaD for precursors of all charge states.

ETD Parameter Evaluation—Electron transfer dissociation results from the reaction of multiply charged precursor cations with appropriate anionic reagents and is generally performed within the confines of a quadrupole ion trap. Optimal performance of ETD is strongly dependent on ion population (both cation and anion), precursor and reagent isolation (prior to reaction), and reaction duration. Here we examine each of these variables and their respective impact on ETD outcomes.

Most published works on ETD use a negative chemical ionization (NCI) source for reagent anion generation (1–6, 15, 33), although dual atmospheric pressure sources have been reported (34–36). However the anions are generated, a critical requirement is that they have a high propensity to donate electrons to the precursor cations rather than abstract protons. Polyaromatic hydrocarbons, such as fluoranthene, have shown good performance in this regard (5, 37). Formation of fluoranthene radical anions in an NCI source, for example, often results in concomitant formation of background anions, many of which engage in proton transfer ion/ion chemistry. Thus, a key step of an ETD experiment is the purification of

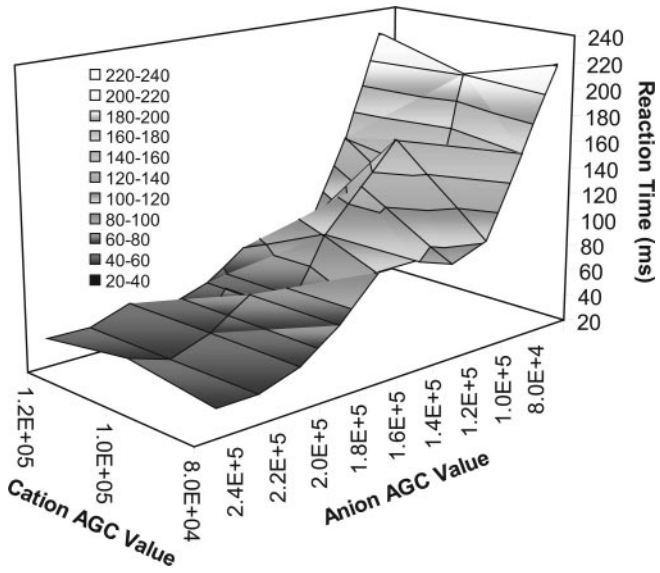

FIG. 5. **The magnitude of both the cation and anion population can substantially affect the optimal ETD reaction time.** Here we plot the reaction duration (ms) at which the maximum product ion population was observed with varying sized cationic and anionic populations. As the population of reagent anions increases, the time to reach the maximum product ion intensity decreases; however, this trend levels off upon reaching the anion storage capacity limit of the ion trap (~200,000 in this experiment).

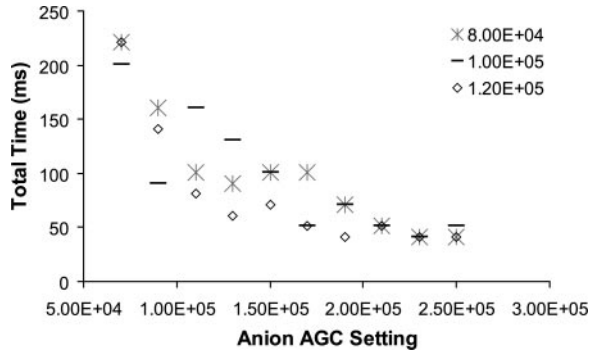

FIG. 6. **Total ion/ion experiment time (sum of the optimal reaction duration and the anion injection time) as a function of anion AGC target value.** These data indicate that the benefit of increased reaction rate outweighs the slightly heightened anion injection durations required to build a larger anion population.

the reagent anion population. The multisegmented QLT system used here utilizes a quadrupole mass filter to transport selected anions from the NCI source to the QLT. Such operation prevents low level anionic contaminants from lowering the apparent electron transfer efficiency with proton transfer side reactions (38–41).

Scan time and duty cycle are key figures of merit for most proteomics experiments especially when performing on-line separations with data-dependent tandem MS where fast scan times are required to adequately sample co-eluting peptides (42). Ideally ETD reactions are accomplished rapidly (<50 ms) and have sufficient efficiency so as not to require spectral averaging. First we evaluated the role of ion density and ion/ion reaction duration on downstream spectral quality and scan times. Fig. 5 displays the effect of ion density (cation and anion) on ETD reaction rate for dissociation of a triply protonated precursor cation. This figure plots the reaction duration at which the maximum product ion intensity was measured for a given anion and cation population (controlled by AGC; see above). As expected from published ion/ion rate models, increasing anion density reduces the required reaction duration (43). In practice, however, space charge effects limit the ion capacity of the trap (44). These data indicate that this threshold is reached at an anion AGC target value of ~200,000; no apparent reduction in reaction time was observed past this amount. Each of the three cation AGC target values resulted in nearly identical optimal reaction durations for the anion densities examined. From these data, we conclude that once an excess amount of reagent anions is established slight variations in the cation densities are negligible (use of cation AGC target values greater than ~120,000 is not practical; see below). Next we considered the trade-off between longer anion injection times (necessary for high AGC values) *versus* the resultant shortened reaction durations. Fig. 6 displays the total ion/ion experiment time (sum of the optimal reaction time and the anion injection time) as a function of anion AGC target value. Largely due to the high flux of anions from the NCI source, the benefit of increased reaction rates greatly outweighs the slightly heightened anion injection periods associated with higher anion AGC target values. Note that ion/ion reaction rates are highly dependent on precursor charge; work is presently ongoing in our laboratory to determine optimal reaction times for all charge states. Regardless of precursor charge, these data suggest that the best ETD performance is achieved when the ion trap is operated at or near its anion space charge capacity.

The space charge limit for storage (anions) in the QLT is much higher than for mass analysis (cations) (45). The magnitude of the cation population is critical: too many will produce space charge-associated mass shifts, whereas too few will result in low product ion intensities and may necessitate spectral averaging (Fig. 7). Fig. 7, *Panels B–D*, display single scan ETD tandem mass spectra of a triply protonated peptide (DRVYIHPFHL) for an AGC cation target population of 5000, 80,000, and 140,000, respectively. Spectra collected at low target values (Fig. 7, *Panel B*) are characterized by poorly defined isotopic cluster peaks, necessitating spectral averaging. Operation with larger target populations produces single scan spectra of much higher quality (Fig. 7, *Panels C* and *D*); however, space charge-associated mass shifts become evident. Fig. 7, *Panel D*, displays an *inset* of the c_2 product ion *m/z* region for eight varying cation AGC target values. For our work we elected to use AGC target settings of ~80,000. Such operation typically generates high quality, single scan ETD spectra with c- and z-type product ion mass shifts less than

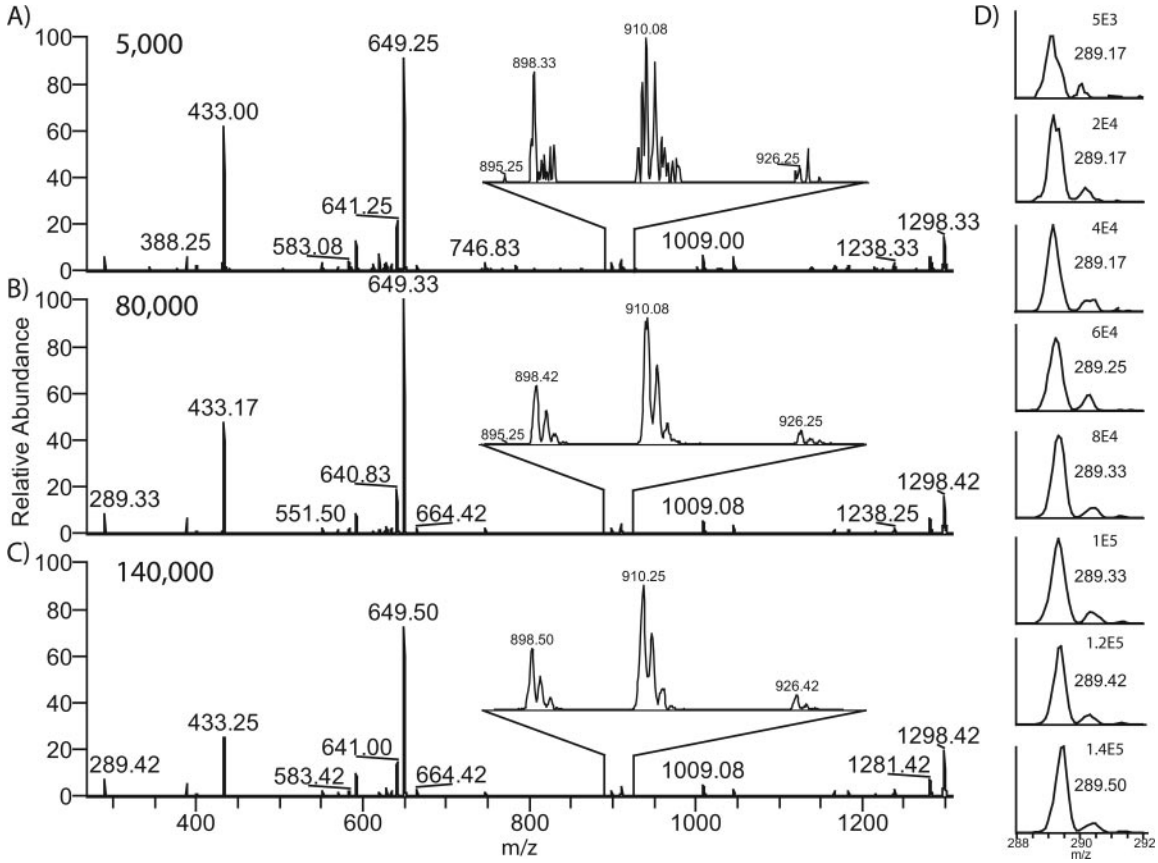

FIG. 7. Shown are the single scan ETD product ion mass spectra of the triply protonated peptide DRVYIHPFHL resulting from a 100-ms reaction with a fixed population of reagent anions (100,000) with varying populations of precursor cations (*Panel A*, 5000; *Panel B*, 80,000; *Panel C*, 140,000). *Panel D* shows the *m/z* region of the c2 fragment (*m/z* 289.16) generated with varying cation precursor populations (5000–140,000). Note the poorly defined isotopic cluster at the 5000 precursor target value and the space charge-induced mass shift at higher cation populations.

0.2 *m/z* units. Note that similar trade-offs between spectral quality and space charge-induced mass shifts exist when performing CAD-type fragmentation; however, because ETD results from an ion/ion reaction, optimal target values are larger (2–3 times as compared with CAD) and highly dependent on both reaction duration and a regulated anion population.

DISCUSSION

With the development of multiple ETD-capable commercial MS systems, the widespread implementation of ETD for various proteomics applications is imminent. Unlike CAD fragmentation, optimal electron transfer reactions require close attention to a number of parameters. Among these parameters, we demonstrated that anion purity, cation and anion AGC target values, and ion/ion reaction duration are the most critical. We also performed a large scale study of ETD performance for small- to medium-sized peptide sequence analysis. These results indicate relatively little overlap in peptide identifications between ion trap CAD and ETD (~12%). ETD outperformed CAD for all charge states greater than 2; however, regardless of precursor charge a linear decrease in percent fragmentation was observed with ETD fragmentation. Our data suggest that a direct correlation exists between the percent fragmentation and ratio of residues per charge. As this number increases so does the probability of intramolecular non-covalent interactions that can bind a newly formed c/z-type ion pair. We applied a recently developed supplemental activation approach (ETcaD) to remedy this problem by converting the non-dissociative ET product ions to useful c- and z-type ions. Automated implementation of such methods should remove this apparent precursor *m/z* ceiling. In this largest scale study of ETD to date, ETD continues to show great promise to propel the field of proteomics. For now, we conclude that ETD provides, at minimum, a highly complementary approach to CAD for peptide sequence analysis.

Acknowledgments—We thank Michael Sussman, Adrian Hegeman, and Edward Huttlin for preparation of the *Arabidopsis* complex protein mixture and Don Hunt and Dina Bai for use of scan sorting software. Finally we thank John Syka and Jae Schwartz for helpful discussions.

* This work was supported in part by the University of Wisconsin-Madison, Thermo Fisher, and National Institutes of Health Grant

1R01GM080148 (to J. J. C.). The costs of publication of this article were defrayed in part by the payment of page charges. This article must therefore be hereby marked "*advertisement*" in accordance with 18 U.S.C. Section 1734 solely to indicate this fact.

S The on-line version of this article (available at http://www.mcponline.org) contains supplemental material.

§ Supported by a National Institutes of Health predoctoral fellowship (Biotechnology Training Program Grant NIH 5T32GM08349).

‖ To whom correspondence should be addressed: Depts. of Chemistry and Biomolecular Chemistry, 1101 University Ave., University of Wisconsin, Madison, WI 53706. Tel.: 608-263-1718; E-mail: jcoon@chem.wisc.edu.

REFERENCES

1. Coon, J. J., Syka, J. E. P., Shabanowitz, J., and Hunt, D. F. (2005) Tandem mass spectrometry for peptide and protein sequence analysis. *Biotechniques* **38,** 519, 521, 523
2. Good, D. M., and Coon, J. J. (2006) Advancing proteomics with ion/ion chemistry. *BioTechniques* **40,** 783–789
3. Mikesh, L. M., Ueberheide, B., Chi, A., Coon, J. J., Syka, J. E. P., Shabanowitz, J., and Hunt, D. F. (2006) The utility of ETD mass spectrometry in proteomic analysis. *Biochim. Biophys. Acta* **1764,** 1811–1822
4. Coon, J. J., Ueberheide, B., Syka, J. E. P., Dryhurst, D. D., Ausio, J., Shabanowitz, J., and Hunt, D. F. (2005) Protein identification using sequential ion/ion reactions and tandem mass spectrometry. *Proc. Natl. Acad. Sci. U. S. A.* **102,** 9463–9468
5. Coon, J. J., Syka, J. E. P., Schwartz, J. C., Shabanowitz, J., and Hunt, D. F. (2004) Anion dependence in the partitioning between proton and electron transfer in ion/ion reactions. *Int. J. Mass Spectrom.* **236,** 33–42
6. Syka, J. E. P., Coon, J. J., Schroeder, M. J., Shabanowitz, J., and Hunt, D. F. (2004) Peptide and protein sequence analysis by electron transfer dissociation mass spectrometry. *Proc. Natl. Acad. Sci. U. S. A.* **101,** 9528–9533
7. Hogan, J. M., Pitteri, S. J., Chrisman, P. A., and McLuckey, S. A. (2005) Complementary structural information from a tryptic N-linked glycopeptide via electron transfer ion/ion reactions and collision-induced dissociation. *J. Proteome Res.* **4,** 628–632
8. Ferguson, P. L., and Smith, R. D. (2003) Proteome analysis by mass spectrometry. *Annu. Rev. Biophys. Biomol. Struct.* **32,** 399–424
9. Wysocki, V. H., Tsaprailis, G., Smith, L. L., and Breci, L. A. (2000) Special feature: Commentary—Mobile and localized protons: a framework for understanding peptide dissociation. *J. Mass Spectrom.* **35,** 1399–1406
10. Tsaprailis, G., Nair, H., Somogyi, A., Wysocki, V. H., Zhong, W. Q., Futrell, J. H., Summerfield, S. G., and Gaskell, S. J. (1999) Influence of secondary structure on the fragmentation of protonated peptides. *J. Am. Chem. Soc.* **121,** 5142–5154
11. Smith, L. L., Herrmann, K. A., and Wysocki, V. H. (2006) Investigation of gas phase ion structure for proline-containing b_2 ion. *J. Am. Soc. Mass Spectrom.* **17,** 20–28
12. Huang, Y. Y., Triscari, J. M., Tseng, G. C., Pasa-Tolic, L., Lipton, M. S., Smith, R. D., and Wysocki, V. H. (2005) Statistical characterization of the charge state and residue dependence of low-energy CID peptide dissociation patterns. *Anal. Chem.***77,** 5800–5813
13. Pitteri, S. J., Chrisman, P. A., Hogan, J. M., and McLuckey, S. A. (2005) Electron transfer ion/ion reactions in a three-dimensional quadrupole ion trap: reactions of doubly and triply protonated peptides with $SO_2^{\cdot-}$. *Anal. Chem.* **77,** 1831–1839
14. Pitteri, S. J., Chrisman, P. A., and McLuckey, S. A. (2005) Electron-transfer ion/ion reactions of doubly protonated peptides: effect of elevated bath gas temperature. *Anal. Chem.* **77,** 5662–5669
15. Swaney, D. L., McAlister, G. C., Wirtala, M., Schwartz, J. C., Syka, J. E. P., and Coon, J. J. (2007) Supplemental activation method for high-efficiency electron-transfer dissociation of doubly protonated peptide precursors. *Anal. Chem.* **79,** 477–485
16. Horn, D. M., Ge, Y., and McLafferty, F. W. (2000) Activated ion electron capture dissociation for mass spectral sequencing of larger (42 kDa) proteins. *Anal. Chem.* **72,** 4778–4784
17. Breuker, K., Oh, H. B., Horn, D. M., Cerda, B. A., and McLafferty, F. W. (2002) Detailed unfolding and folding of gaseous ubiquitin ions characterized by electron capture dissociation. *J. Am. Chem. Soc.* **124,** 6407–6420
18. Horn, D. M., Breuker, K., Frank, A. J., and McLafferty, F. W. (2001) Kinetic intermediates in the folding of gaseous protein ions characterized by electron capture dissociation mass spectrometry. *J. Am. Chem. Soc.* **123,** 9792–9799
19. Tsybin, Y. O., Witt, M., Baykut, G., Kjeldsen, F., and Hakansson, P. (2003) Combined infrared multiphoton dissociation and electron capture dissociation with a hollow electron beam in Fourier transform ion cyclotron resonance mass spectrometry. *Rapid Commun. Mass Spectrom.* **17,** 1759–1768
20. Mihalca, R., van der Burgt, Y. E. M., McDonnell, L. A., Duursma, M., Cerjak, I., Heck, A. J. R., and Heeren, R. M. A. (2006) Combined infrared multiphoton dissociation and electron-capture dissociation using collinear and overlapping beams in Fourier transform ion cyclotron resonance mass spectrometry. *Rapid Commun. Mass Spectrom.* **20,** 1838–1844
21. Martin, S. E., Shabanowitz, J., Hunt, D. F., and Marto, J. A. (2000) Subfemtomole MS and MS/MS peptide sequence analysis using nano-HPLC micro-ESI Fourier transform ion cyclotron resonance mass spectrometry. *Anal. Chem.* **72,** 4266–4274
22. Geer, L. Y., Markey, S. P., Kowalak, J. A., Wagner, L., Xu, M., Maynard, D. M., Yang, X. Y., Shi, W. Y., and Bryant, S. H. (2004) Open mass spectrometry search algorithm. *J. Proteome Res.* **3,** 958–964
23. Elias, J. E., and Gygi, S. P. (2007) Target-decoy search strategy for increased confidence in large-scale protein identifications by mass spectrometry. *Nat. Methods* **4,** 207–214
24. Iavarone, A. T., Paech, K., and Williams, E. R. (2004) Effects of charge state and cationizing agent on the electron capture dissociation of a peptide. *Anal. Chem.* **76,** 2231–2238
25. Zubarev, R. A., Horn, D. M., Fridriksson, E. K., Kelleher, N. L., Kruger, N. A., Lewis, M. A., Carpenter, B. K., and McLafferty, F. W. (2000) Electron capture dissociation for structural characterization of multiply charged protein cations. *Anal. Chem.* **72,** 563–573
26. Tsybin, Y. O., Haselmann, K. F., Emmett, M. R., Hendrickson, C. L., and Marshall, A. G. (2006) Charge location directs electron capture dissociation of peptide dications. *J. Am. Soc. Mass Spectrom.* **17,** 1704–1711
27. Belyayev, M. A., Cournoyer, J. J., Lin, C., and O'Connor, P. B. (2006) The effect of radical trap moieties on electron capture dissociation spectra of substance P. *J. Am. Soc. Mass Spectrom.* **17,** 1428–1436
28. Chakraborty, T., Holm, A. I. S., Hvelplund, P., Nielsen, S. B., Poully, J. C., Worm, E. S., and Williams, E. R. (2006) On the survival of peptide cations after electron capture: Role of internal hydrogen bonding and microsolvation. *J. Am. Soc. Mass Spectrom.* **17,** 1675–1680
29. Lin, C., O'Connor, P. B., and Cournoyer, J. J. (2006) Use of a double resonance electron capture dissociation experiment to probe fragment intermediate lifetimes. *J. Am. Soc. Mass Spectrom.* **17,** 1605–1615
30. Robinson, E. W., Leib, R. D., and Williams, E. R. (2006) The role of conformation on electron capture dissociation of ubiquitin. *J. Am. Soc. Mass Spectrom.* **17,** 1469–1479
31. Zubarev, R. A., Kelleher, N. L., and McLafferty, F. W. (1998) Electron capture dissociation of multiply charged protein cations. A nonergodic process. *J. Am. Chem. Soc.* **120,** 3265–3266
32. Stein, S. E. (1999) An integrated method for spectrum extraction and compound identification from gas chromatography/mass spectrometry data. *J. Am. Soc. Mass Spectrom.* **10,** 770–781
33. Schroeder, M. J., Webb, D. J., Shabanowitz, J., Horwitz, A. F., and Huntt, D. F. (2005) Methods for the detection of paxillin post-translational modifications and interacting proteins by mass spectrometry. *J. Proteome Res.* **4,** 1832–1841
34. Huang, T. Y., Emory, J. F., O'Hair, R. A. J., and McLuckey, S. A. (2006) Electron-transfer reagent anion formation via electrospray ionization and collision-induced dissociation. *Anal. Chem.* **78,** 7387–7391
35. Liang, X. R., Xia, Y., and McLuckey, S. A. (2006) Alternately pulsed nano-electrospray ionization/atmospheric pressure chemical ionization for ion/ion reactions in an electrodynamic ion trap. *Anal. Chem.* **78,** 3208–3212
36. Xia, Y., Liang, X. R., and McLuckey, S. A. (2005) Pulsed dual electrospray ionization for ion/ion reactions. *J. Am. Soc. Mass Spectrom.* **16,** 1750–1756
37. Gunawardena, H. P., He, M., Chrisman, P. A., Pitteri, S. J., Hogan, J. M.,

Hodges, B. D. M., and McLuckey, S. A. (2005) Electron transfer versus proton transfer in gas-phase ion/ion reactions of polyprotonated peptides. *J. Am. Chem. Soc.* **127,** 12627–12639
38. He, M., and McLuckey, S. A. (2004) Charge permutation reactions in tandem mass spectrometry. *J. Mass Spectrom.* **39,** 1231–1259
39. Reid, G. E., Shang, H., Hogan, J. M., Lee, G. U., and McLuckey, S. A. (2002) Gas-phase concentration, purification, and identification of whole proteins from complex mixtures. *J. Am. Chem. Soc.* **124,** 7353–7362
40. McLuckey, S. A., and Stephenson, J. L. (1998) Ion ion chemistry of high-mass multiply charged ions. *Mass Spectrom. Rev.* **17,** 369–407
41. McLuckey, S. A., Stephenson, J. L., and Asano, K. G. (1998) Ion/ion proton-transfer kinetics: implications for analysis of ions derived from electrospray of protein mixtures. *Anal. Chem.* **70,** 1198–1202
42. Aebersold, R., and Mann, M. (2003) Mass spectrometry-based proteomics. *Nature* **422,** 198–207
43. Stephenson, J. L., and McLuckey, S. A. (1996) Ion/ion reactions in the gas phase: Proton transfer reactions involving multiply-charged proteins. *J. Am. Chem. Soc.* **118,** 7390–7397
44. Cox, K. A., Cleven, C. D., and Cooks, R. G. (1995) Mass shifts and local space-charge effects observed in the quadrupole ion-trap at higher resolution. *Int. J. Mass Spectrom. Ion Process.* **144,** 47–65
45. Schwartz, J. C., Senko, M. W., and Syka, J. E. P. (2002) A two-dimensional quadrupole ion trap mass spectrometer. *J. Am. Soc. Mass Spectrom.* **13,** 659–669